inter.noise 2014
MELBOURNE AUSTRALIA
16-19 NOVEMBER

Interaction of a pair of horizontally aligned bubbles in gravity field

Han JIAO[1]; Dongyan SHI[2]; Zhikai Wang[3]; Hongqun LI[4]

[1] Harbin Engineering University, China

[2] Harbin Engineering University, China

[3] Harbin Engineering University, China

[4] Harbin Engineering University, China

ABSTRACT

Both large deformation and strong discontinuity problems exist in the process of bubble-bubble interaction. The lattice Boltzmann method which is based on the microscopic level has naturally comparative advantage to describe tiny changes in multiphase flow system. A three-dimensional lattice Boltzmann (LB) model of two horizontally aligned bubbles is presented to explore the bubble movement, topological transformation and bubbles interaction characteristics. In this model, the viscous effect is easily considered, and surface tension effect is realized by introducing a discrete LB body force term. To provide a reference, the isolated bubble dynamics driven by gravity is simulated firstly, and the surface tension effect is studied. Then the effect of gap distance and interface width on the coalescence of two stable bubbles is discussed. Finally, the interaction of two horizontal bubbles with different size ratio in gravity field is explored carefully. The results not only show the detailed coupling and coalescence process of two rising bubbles, but expose that the relative size ratio plays an important role in the interaction. The opposite phenomenon can be seen. When bubbles are of different size, the coalescence phenomenon will happen, but when they are in the same size, the rejection phenomenon will replace it.

Keywords: Horizontal bubbles, Interaction, Lattice Boltzmann method
I-INCE Classification of Subjects Number(s): 21.6

1. INTRODUCTION

Bubble group plays an important role in the hydrodynamic characteristics of the surrounding fluid flow, especially affects some sophisticated underwater equipment, such as propeller. Their collective collapse phenomenon is one of the main sources of structure vibration and underwater noise (1-3). Thus, it is quite necessary to study the interaction mechanism of bubbles. At present, the studies of single-bubble movement in gravity field, including shapes and floating velocity, already have relatively adequate outcomes (4-6). By contrast, cases about multi-bubble motion characteristics which are closer to the actual engineering are relatively rare. When there is an another bubble in the vicinity of a bubble, interactions can cause remarkable changes of the flow field properties and the movement of bubbles, including bubble breakup and fusion (7-9).

In 1996, Katz et al. (10) found that bubbles in a pipe will produce collisions under the action of the vortex at the Reynolds number between 0.2 and 35. In 1999, Krishna et al. (11) considered the coupling effect between small and large bubbles. In 2009, Sanada et al. (12) observed the interaction between a pair of horizontally bubbles by using the high-speed photography, and found the fusion and rebounding phenomena. In 2012, Zhang A M. et al. (13) studied the fusion of two horizontal bubbles near the free surface. Compared with experimental research, numerical simulation owns advantages of controllable environment, accurate setting parameter and observable results. In 2003, the distribution of velocity and vortex around the bubble surface were successfully obtained by Legendre et al. with the body-fitted grid

[1] jiaohan199203@gmail.com
[2] shidongyan@hrbeu.edu.cn
[3] zhikai.wa@gmail.com
[4] lihongqun@hrbeu.edu.cn

technology. In 2010, Rabha and Buwa et al. (14) discussed the interaction of bubbles in shear flow by using the VOF method.

Lattice Boltzmann Method (LBM) is another relatively new developed numerical method. Compared with traditional numerical methods, this method, which is of the microscopic properties and ease of programming, can achieve the second-order accuracy requirement in simulating single-phase flows (15, 16), and multiphase flows (9,17). At present, this method mainly includes the color model, the potential field model and the free energy model. Different from the other two models, the free energy model can ensure the thermodynamic consistency (18). In this paper, the horizontal two bubble interaction model in free field is established based on this model. The process to verify the two bubble interaction model is divided into two parts: an isolated bubble in gravity field and two bubble interaction crossly affected by the bubble wall thickness and the gap distance (18) unconsidering gravity. Finally, the coupling characteristics of a pair of bubbles laid side by side were explored on the terms of the relative position and the relative size, respectively. The implemented of lattice Boltzmann method in simulating bubble dynamics is briefly described in Section 2, while the simulation results are presented in Section 3. Finally, the conclusion is provided in Section 4.

2. NUMERICAL METHOD

2.1 Governing Equation

The governing equations to describe bubble dynamics in non-Newtonian viscous flow field can be written as (4, 19),

$$\begin{cases} \partial\rho/\partial t+\nabla\cdot(\rho\mathbf{u})=0 \\ \partial(\rho\mathbf{u})/\partial t+\nabla\cdot(\rho\mathbf{u}\mathbf{u})=-\nabla\cdot\mathbf{P}+\mu\nabla^2\mathbf{u}+\mathbf{F} \\ \partial\Psi/\partial t+\nabla\cdot(\Psi\mathbf{u})=\Upsilon_M\nabla^2\mu_\Psi \end{cases}. \quad (1)$$

Where, the first two equations are the Navier-Stokes equations and the third one is the Cahn-Hilliard equation. ρ, $\mathbf{u}$ and $\mathbf{P}$ are density, velocity and pressure. Initially, to describe two-phase particles movement uniformly, ρ_0 is defined as $\rho_0=(\rho_H+\rho_L)/2$, where ρ_H and ρ_L denote the density of liquid and gas respectively. F is the body force. Ψ denotes an order parameter to capture the two-phase interface, $\Psi_0=(\rho_H-\rho_L)/2$. Υ_M is the mobility rate. μ_Ψ is defined for calculating the surface tension (18).

$$\mu_\Psi=12\sigma(\Psi^3-\Psi\Psi_0^2)/W\Psi_0^4-3\sigma W/2\Psi_0^2. \quad (2)$$

Where σ is the surface tension coefficient, W is the thickness of the bubble wall.

2.2 Lattice Boltzmann Method

To recover the Navier-Stokes equations and the Cahn-Hilliard equation, two groups of lattice Boltzmann equations are constructed (4, 20),

$$f_i(\mathbf{r}+\mathbf{c}_i\delta_t,t+\delta_t)-f_i(\mathbf{r},t)=[f_i^{(eq)}(\mathbf{r},t)-f_i(\mathbf{r},t)]/\tau_\rho. \quad (3)$$

$$g_i(\mathbf{r}+\mathbf{c}_i\delta_t,t+\delta_t)-g_i(\mathbf{r},t)=(1-q)\left[g_i(\mathbf{r}+\mathbf{c}_i\delta_t,t)-g_i(\mathbf{r},t)\right]+[g_i^{(eq)}(\mathbf{r},t)-g_i(\mathbf{r},t)]/\tau_\Psi. \quad (4)$$

$f_i(\mathbf{r},t)$ and $g_i(\mathbf{r},t)$ are number density of the particle distribution at a local position in the certain time. By multi-scale expansion, Eq. (2) can obtain the Navier-Stokes equations while Eq. (3) can get the Cahn-Hilliard equation with second-order accuracy. q is the control coefficient, $q=\dfrac{1}{\tau_\Psi+0.5}$. $\mathbf{c}_i$ denotes discrete velocities depending on the lattice structure. To improve the computational efficiency, D3Q19 and D3Q7 models are separately adopted in Eq. (3) and (4).

$$\begin{cases} \mathbf{c}_i=(0,0,0)dx/dt, i=0 \\ \mathbf{c}_i=(\pm1,0,0)dx/dt,(0,\pm1,0)dx/dt,(0,0,\pm1)dx/dt, i=1\sim6 \\ \mathbf{c}_i=(\pm1,\pm1,0)dx/dt,(\pm1,0,\pm1)dx/dt,(0,\pm1,\pm1)dx/dt, i=7\sim18 \end{cases}. \quad (5)$$

The distribution of nineteen discrete velocities in D3Q19 is shown in Eq. (5), and the discrete velocity distribution in D3Q7 is just the first seven discrete velocities in Eq. (5). τ_ρ and τ_Ψ are the relaxation coefficients, and τ_ρ is associated with μ. c_s is lattice sound velocity, $c_s=1/\sqrt{3}$.

The equilibrium density functions, $f_i^{(eq)}, g_i^{(eq)}$, come from the Max-well distribution (9),

$$f_i^{(eq)} = \begin{cases} w_i[\rho(1-3\mathbf{u}/2) - 6\Psi\mu_\Psi], i=0 \\ w_i[\rho(1+3\mathbf{c}_i\cdot\mathbf{u} + 9(\mathbf{c}_i\mathbf{u})^2/2 - 3\mathbf{u}^2/2) + 3\Psi\mu_\Psi], i=1\sim 18 \end{cases}, \tag{6}$$

$$g_i^{(eq)} = \begin{cases} -3(\Gamma\mu_\Psi + c_s^2\Psi), i=0 \\ [2\Gamma\mu_\Psi + (2\tau_\Psi+1)(\mathbf{c}_i\cdot\mathbf{u})\Psi]/4, i=1\sim 6 \end{cases}. \tag{7}$$

where w_i is the weight coefficient in the each discrete direction. w_0= 4/9, $w_{1\sim6}$= 1/9, $w_{7\sim18}$= 1/36. Γ is used to control the mobility ratio and is related to the parameter Υ_Ψ in Eq. (1) (18)

$$\Upsilon_\Psi = (2\tau_\Psi - 1)/(2\tau_\Psi + 1)\Gamma. \tag{8}$$

In order to accurately introduce the body force F in Eq. (1) as a lattice form, the discrete scheme proposed by Guo Z. L. et al. (21) is adopted in this paper,

$$\mathbf{F}_i = 3w_i(1-1/2\tau_\rho)[(\mathbf{c}_i - \mathbf{u}) + 3(\mathbf{c}_i\cdot\mathbf{u})\mathbf{c}_i]\cdot\mathbf{F}. \tag{9}$$

Meanwhile, combining with the sub-step operation of Lee T. et al. (22), via introducing an intermediate variable g_i^{mid}, the traditional single-step collision operation is transformed into two steps, making the model more flexibility. The expression is as follows,

$$\begin{cases} g_i^{mid}(\mathbf{r},t) = g_i(\mathbf{r},t) + (g_i^{(eq)}(\mathbf{r},t) - g_i(\mathbf{r},t))/\tau_\Psi \\ g_i(\mathbf{r}+\mathbf{c}_i\delta_t, t+\delta_t) = (1-1/(\tau_\Psi+0.5))g_i^{(eq)}(\mathbf{r}+\mathbf{c}_i\delta_t,t) + 1/(\tau_\Psi+0.5)g_\Psi^{mid}(\mathbf{r},t) \end{cases}. \tag{10}$$

The macroscopic fluid parameters, like the density ρ and the velocity **u** and the order parameter Ψ, can be calculated from

$$\begin{cases} \rho = \sum_{i=0}^{18} f_i \\ \mathbf{u} = [\sum_{i=0}^{18} f_i\mathbf{c}_i + (\mu_\Psi\nabla\Psi + \mathbf{F})/2]/\rho \\ \Psi = \sum_{i=0}^{6} g_i \end{cases}. \tag{11}$$

3. RESULTS AND DISCUSSION

3.1 Isolated Rising Bubble

To explore the bubble behavior and the interaction characteristics of two horizontally arranged bubbles in gravity field, the isolated bubble was firstly simulated to confirm the ability of the model to capture the multiphase interface. The fluid properties can be districted by the latter three parameters (9),

$$Mo = \frac{(\rho_H - \rho_L)g}{\sigma^3\rho_H^2}\cdot\mu_H^4, Eo = \frac{(\rho_H-\rho_L)g}{\sigma}\cdot D^2, \mathrm{Re} = \frac{\rho u D}{2}. \tag{12}$$

Here, g stands for the gravity, μ_H is the viscosity parameter of the fluid component, D is the diameter of the bubble, and the other parameters are the same with those defined before.

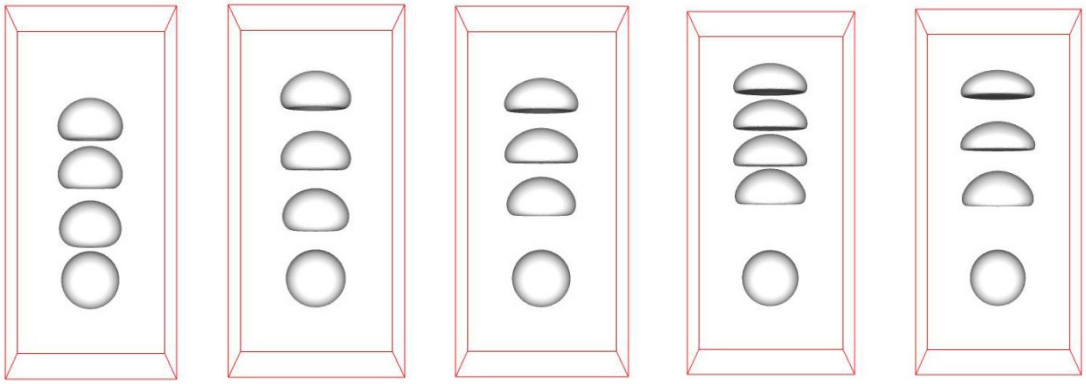

(a) (b) (c) (d) (e)

Figure 1 – The rising process of a bubble with different surface tension coefficient in gravity field. (a) $\sigma = 0.1$, (b) $\sigma = 0.2$, (c) $\sigma = 0.5$, (d) $\sigma = 1.0$, (e) $\sigma = 2.0$

In the simulation, $\rho_H = 1000$, $\rho_L = 1$, $\tau_\rho = 0.6$, $\tau_\delta = 0.7$, $\Gamma = 400$, $D = 2R = 40$. *Mo* and *Eo* are changed according to the modified surface tension coefficient σ. Figure 1 shows the rising process and the terminal shape with different surface tension coefficient. The simulation results can verify the newly built model in the paper in two aspects: (1) the large deformation of the multiphase surface; (2) the terminal shape agrees well with the observation by Bhaga D. (5), and the trend of terminal shape changing along the value of *Mo* is same with that in the literature (23) where the terminal shape becomes more platter with smaller *Mo*.

3.2 Two Horizontally Steady Bubbles

To identify the model in dealing with multi-bubble interaction, the crossing effect of bubble wall width and gap distance on the interaction characteristics is studied by simulating two bubble in static flow. For a comparative analysis, the parameters are valued according to the literature (18). The two bubbles are with the same radius $R = 20\,\delta_l$, and the gap distance, $d = 5.0\,\delta_l$. The parameters are chosen as, $\sigma = 1.0$, $\tau_\rho = 0.6$, $\tau_\delta = 0.7$, $\Gamma = 400$, and the bubble wall width, W is modified. The periodic boundary condition is employed at all boundaries.

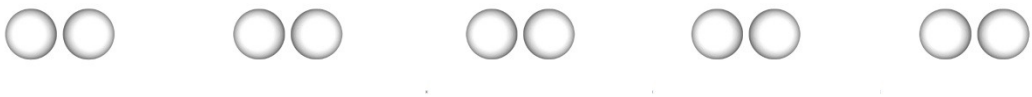

(a) (b) (c) (d) (e)

Figure 2 – Results of two stationary bubbles ($W = 2.4\,\delta_l$). (a) $t = 0$; (b) $t = 2.21$; (c) $t = 2.37$; (d) $t = 2.69$; (e) $t = 3.0$

(a) (b) (c) (d) (e)

Figure 3 – Results of two stationary bubbles ($W = 2.6\,\delta_l$). (a) $t = 0$; (b) $t = 2.21$; (c) $t = 2.37$; (d) $t = 2.69$; (e) $t = 3.0$

At first, W is set as 2.4. That is, the gap distance is greater than $2W$. Numerical results are shown in Figure 2. It can be easily observed that the two bubbles do not merge or even have the trend. Then, W is set as 2.6, which means that the gap distance is less than $2W$. Other parameters remain unchanged. Numerical results are shown in Fig. 3. The coalescence process can be easily observed. The results are consistent with

the conclusion that the coalescence phenomenon only happens when the gap distance is less than $2W$, which is first drew by Zheng H. W. (18) by using a two dimensional lattice Boltzmann model.

3.3 Two Horizontally Rising Bubbles

Keeping the gap distance and the bubble wall width stable, the coalescence processes with the radius ratio of 1:1, 4:3, 2:1 are studied respectively. The periodic boundaries are used for all boundaries, and to remove the influence of the boundaries, the initial distance between the boundary and the bubble center is set as four times as the bubble radius. The other parameters are set as Eo =39.96, σ =1.0, τ_ρ =0.6, τ_ϕ =0.7, Γ =400 and W =2.6 δ_l .

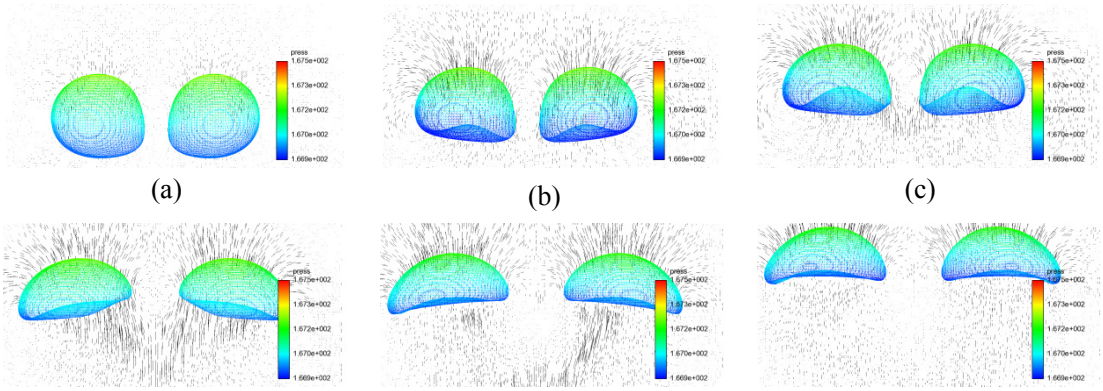

Figure 4 – Movement trajectory of two horizontal bubbles with the same size. (a) t = 0.79; (b) t = 1.58; (c) t = 2.21; (d) t = 3.79; (e) t = 4.74; (f) t = 6.32.

The movement trajectory of two horizontal bubbles with the same size, R = 20, is shown in Figure 4. And the pressure pattern and velocity vectors are shown in it. The repulsion phenomenon can be clearly found, but the attraction appears at the initial stage. As the bubbles rise, the surround fluids begin to move and format two vortex rings. The parts of the two vortex rings in the gap seem to be canceled, and repulsive force in the horizontal direction appears. The gap distance becomes bigger and bigger, until the two bubbles can merely influence each other. And each bubble expresses as the dynamics of an isolated bubble rising.

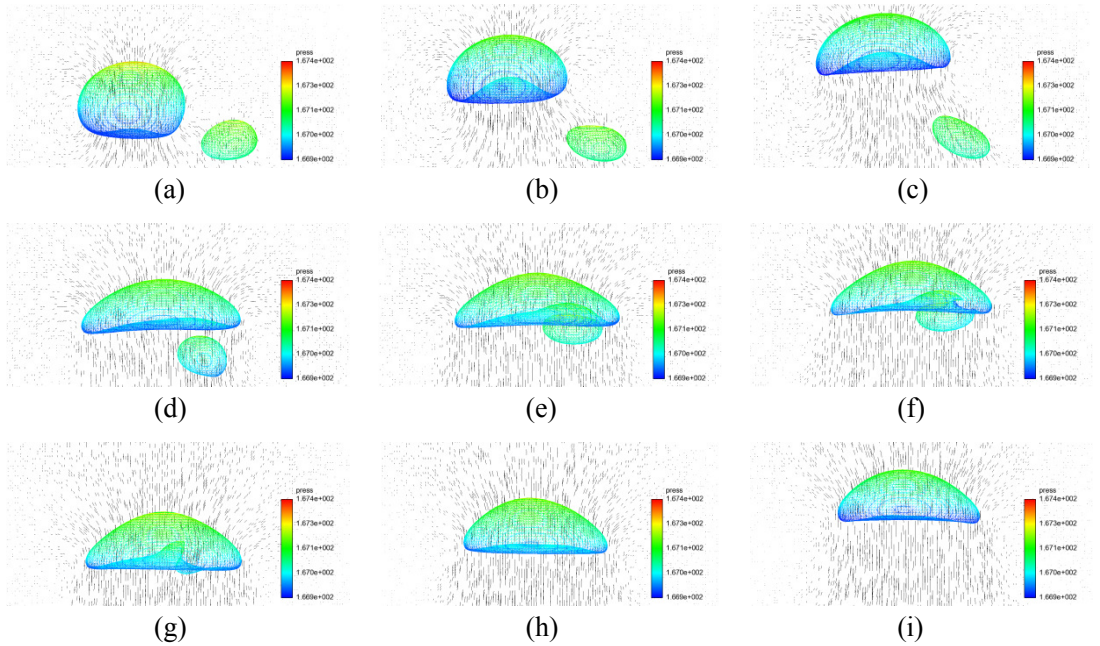

Figure 5 – Coalescence process of two horizontal bubbles with R_1:R_2 = 2:1. (a) t = 0.79; (b) t = 1.58; (c) t = 2.37; (d) t = 4.74; (e) t = 7.12; (f) t = 7.91; (g) t = 8.70; (h) t = 10.28; (i) t = 11.07.

Figure 5 shows the coalescence process of two horizontal bubbles with R_1:R_2 = 2:1. After the bubbles are released, the bigger bubble goes faster, and the gap distance increases at first. As the vortex appears, the smaller bubble movement is influenced by both gravity and the vortex. When it

comes into the wake of the bigger bubble, the gap distance decreases quickly. At about $t = 7.12$, a slight bulge on the button surface of the bigger bubble appears duo to the approach of the smaller bubble. The wave motion of the button surface including the surface breaking and rebuilt is shown in Figure 5(f)-(g). After the wave motion comes smooth under the effect of surface tension, the merged bubble keeps rising.

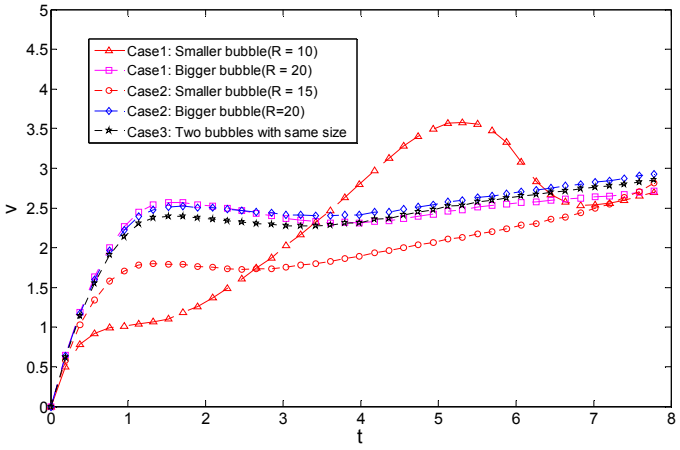

Figure – 6 Comparison of the rising velocity of the two horizontal bubbles with different relative size in the coalescence process.

The rising velocities of the two horizontal bubbles with different relative size in the coalescence process are shown in Figure 6. According to the different radius ratio, the working conditions are classified into three cases: case 1 (R_1:R_2 = 2:1), case 2 (R_1:R_2 = 4:3), and case 3 (R_1:R_2 = 1:1). t is the dimensionless time, and v is the vertical velocity. All curves show that the velocity increases at a faster rate under the effect of gravity in the beginning. Subsequently, the vortex appears, and the velocity of the smaller bubble is suppressed, but that of the bigger bubble is merely influenced. For the bubbles with the same size, their curves completely coincide. It can be found that the variation of velocity matches well with the phenomenon of deformation shown in Figures 4-5. The results also show that the relative size plays an important role in the coalescence process of two horizontal bubbles. The larger the size difference is, the larger the effects of the bigger bubble on the smaller one will be. However, the bigger bubble is barely influenced by the smaller one. And the completely adverse phenomena of coalescence and repulsion appear when two horizontal bubbles have the same size.

To identify the discovery mentioned above and test the initial gap distance effecting on it, more cases are simulated with the working conditions of A-B-C where A, B and C stand for the first bubble radius, the second bubble radius and the initial gap distance respectively. Extraneous three cases are carried out for each radius ratio condition. The more detailed information about the initial condition is listed in table 1.

Table 1 Information about the key velocity and time points

Cases (A-B-C)	t_1	t_2	t_3	t_4	v_1	v_2	v_3
20-20-15	1.52			3.42	2.40		2.25
20-20-8	1.71			3.04	2.39		2.28
20-20-5	1.71			3.03	2.40		2.30
20-15-15	1.71	12.71	9.90	3.42	2.50	5.49	2.37
20-15-8	1.70	9.30	7.34	3.45	2.52	4.80	2.41
20-15-5	1.65	8.35	6.56	3.50	2.53	4.43	2.44
20-10-15	1.61	7.21	4.52	3.98	2.55	3.94	2.30

20-10-8	1.72	4.74	3.11	4.00	2.57	3.46	2.32
20-10-5	1.72	3.80	2.72	3.98	2.58	3.37	2.33

Note: t_1 and t_2 stand for the time point that the bigger and the smaller bubbles firstly get the peak velocity, and t_3 is the time that the velocities of the two bubbles firstly get equality. t_4 is the time that the bigger bubble firstly gets the valley velocity. v_1 and v_2 stand for the first peak velocity of the bigger and the smaller bubbles respectively. v_3 stands for the first valley velocity of the bigger bubble.

Table 1 also shows the information about the key velocity and time points. As shown in the second, sixth and eighth columns, the values do not fluctuate much in different working conditions, which means that the gap distance and the smaller bubble have little effect on the bigger bubble. Comparing with t_2, t_3 and t_4, the results that the relative size has more obvious effect than the gap distance can be indicated. By decreasing the gap distance and increasing the radius ratio, the coalescence process can be accelerated. Combining the third and the seventh columns, it can be clearly seen that as the size difference decreases, the time wasted by the smaller bubble to reach v_2 and the value of v_2 increases. At the same time, keeping the relative size stable, by increasing the initial gap distance can also increase the value of v_2. It can be concluded that both the initial gap distance and the relative size play an important role in the coalescence process, but the latter one may be more obvious. With the radius ratio and the gap distance increasing, the bigger bubble will be less influenced while the small one is influenced seriously.

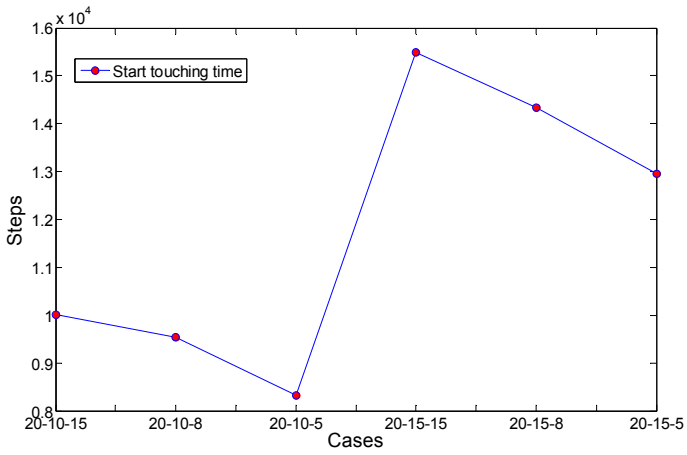

Figure 7 – Time of two horizontal bubbles beginning to touch at different initial conditions (A-B-C)
A is the radius of the bigger bubble, B is the radius of the smaller bubble,
C is the gap distance between the two bubbles.

Figure 7 shows the effects of the relative size coupling with the gap distance on the bubble merging time. It can be found that the whole tendency of the curve is plotted as the shape of an inverse letter 'Z'. It indicates that the difference of their starting touching time is almost proportional to the difference in the initial gap distance. However, the relative size has a greater effect on it.

4. CONCLUSION

Based on the lattice Boltzmann method, a three-dimensional bubble-bubble interaction model considering the surface tension and the gravity is built. By using this model, the interaction of two gravity-driven bubbles horizontally aligned in the viscous flow field is explored. Firstly, two general cases that an isolated bubble rising in gravity field and two stable bubbles interaction unconsidering the gravity are studied to verify the ability of the model in simulating the multiphase interface movement. Then, the effect of radius ratio on the rising process of two horizontally aligned bubbles is researched. Two contrary phenomena, repulsion and coefficient are observed. When the two bubbles are the same size, the repulsion appears. But, the coalescence phenomenon will take the place of it when the size is different. And with the same gap distance, the more the bubbles differ from each other in size, the more easily the two bubbles will merge together. Finally, the effects of the gap distance coupling relative size are researched. It is found that both radius ratio and gas distance play an important role in the interaction. Compared with the radius ratio, the effect of the radius ratio seems weaker. Decreasing the gap distance can do help for the two bubbles

coalescence. During the interaction process, the bigger bubble is merely influenced while the smaller bubble is influenced seriously.

ACKNOWLEDGEMENTS

This paper is funded by the International Exchange Program of Harbin Engineering University for Innovation-oriented Talents Cultivation. And the authors are grateful to the Program of the Scientists Fund for Outstanding Young Scholars of China (Grant No. 51222904) and the Program for New Century Excellent Talents in University (Grant No. NCET100054) for support.

REFERENCES

1. Hsiao CT, Chahine GL. Effect of a propeller and gas diffusion on bubble nuclei distribution in a liquid. J Hydrodyn. 2012; 24(6): 809-822.
2. Zhu Z, Fang S. Numerical investigation of cavitation performance of ship propellers. J Hydrodyn. 2012; 24(3): 347-353.
3. Ji B, Luo X, Peng X. Numerical analysis of cavitation evolution and excited pressure fluctuation around a propeller in non-uniform wake. Int J Multiphas Flow. 2012; 43: 13-21.
4. Amaya-Bower L, Lee T. Single bubble rising dynamics for moderate Reynolds number using lattice Boltzmann method. Comput Fluids. 2010; 39(7): 1191-1207.
5. Bhaga D, Weber ME. Bubbles in viscous liquids: shapes, wakes and velocities. J Fluid Mech. 1981; 105: 61-85.
6. Ohta M, Imura T, Yoshida Y. A computational study of the effect of initial bubble conditions on the motion of a gas bubble rising in viscous liquids. Int J Multiphas Flow. 2005; 31(2): 223-237.
7. Chen RH, Tian WX, Su GH. Numerical investigation on coalescence of bubble pairs rising in a stagnant liquid. Chem Eng Sci. 2011; 66(21): 5055-5063.
8. Yu Z, Yang H, Fan LS. Numerical simulation of bubble interactions using an adaptive lattice Boltzmann method. Chem Eng Sci . 2011; 66(14): 3441-3451.
9. Cheng M, Hua J, Lou J. Simulation of bubble–bubble interaction using a lattice Boltzmann method. Comput Fluids. 2010; 39(2): 260-270.
10. Katz J, Meneveau C. Wake-induced relative motion of bubbles rising in line. Int J Multiphas Flow. 1996; 22(2): 239-258.
11. Krishna R, Urseanu MI, Van Baten JM. Rise velocity of a swarm of large gas bubbles in liquids. Chem Eng Sci. 1999; 54(2): 171-183.
12. Sanada T, Sato A, Shirota M. Motion and coalescence of a pair of bubbles rising side by side. Chem Eng Sci. 2009; 64(11): 2659-2671.
13. Zhang AM, Yao XL. The interaction between multiple bubbles and the free surface. Chinese Phys B. 2008; 17(3): 927.
14. Rabha SS, Buwa VV. Volume-of-fluid (VOF) simulations of rise of single/multiple bubbles in sheared liquids. Chem Eng Sci. 2010; 65(1): 527-537.
15. Åsén PO, Kreiss G, Rempfer D. Direct numerical simulations of localized disturbances in pipe Poiseuille flow. Comput Fluids. 2010; 39(6): 926-935.
16. Higuera FJ, Succi S. Simulating the flow around a circular cylinder with a lattice Boltzmann equation. EPL (Europhysics Lett). 1989; 8(6): 517.
17. Inamuro T, Ogata T, Tajima S. A lattice Boltzmann method for incompressible two-phase flows with large density differences. J Comput Phys. 2004; 198(2): 628-644.
18. Zheng HW, Shu C, Chew YT. A lattice Boltzmann model for multiphase flows with large density ratio. J Comput Phys. 2006; 218(1): 353-371.
19. Shan X, Chen H. Lattice Boltzmann model for simulating flows with multiple phases and components. Phys Rev E. 1993; 47(3): 1815.
20. Qian Y H, d'Humières D, Lallemand P. Lattice BGK models for Navier-Stokes equation. EPL (Europhysics Lett). 1992; 17(6): 479.
21. Guo Z, Zheng C, Shi B. Discrete lattice effects on the forcing term in the lattice Boltzmann method. Phys Rev E. 2002; 65(4): 046308.
22. Lee T, Lin CL. A stable discretization of the lattice Boltzmann equation for simulation of incompressible two-phase flows at high density ratio. J Comput Phys. 2005; 206(1): 16-47.
23. Anwar S. Lattice Boltzmann modeling of buoyant rise of single and multiple bubbles. Comput Fluids. 2013; 88: 430-439.